9

Modeling Variably Saturated Water Flow and Multicomponent Reactive Transport in Constructed Wetlands

Günter Langergraber[1] *and Jirka Šimůnek*[2]

[1] *Institute of Sanitary Engineering and Water Pollution Control, University of Natural Resources and Life Sciences Vienna (BOKU), A-1190, Vienna, Austria*
[2] *Department of Environmental Sciences, University of California Riverside, Riverside, CA, 92521, USA*

9.1 Introduction

Constructed wetlands (CWs) are engineered treatment systems that optimize treatment processes found in natural environments and are therefore considered to be sustainable, environmentally friendly solutions to engineering problems. Processes occurring in CWs are very complex, and include a large number of simultaneously active physical, chemical, and biological processes that mutually influence each other. CWs are systems that efficiently treat different types of polluted water (e.g. Kadlec and Wallace, 2009; García et al., 2010).

For a long time, CWs have been considered 'black boxes'. Little effort has been made to understand the main processes leading to contaminant removal. Still today, most models for wetlands are using a 'black box' approach – they do not consider processes in wetlands in detail. For 'black box' models, data from experiments are needed to derive model equations. In process-based models the mathematical equations are based on processes in wetlands and include balance equations for energy, mass, charge, and so on. Data from experiments are used for calibration and validation of models. Better predictions should be possible using these models (Langergraber, 2011).

When developing a wetland model, a number of different processes have to be considered (Langergraber et al., 2009b):

- the flow model (describing water flow in the porous media);
- the transport model (describing transport of constituents as well as adsorption and desorption processes);
- the biokinetic model (describing biochemical transformation and degradation processes of the constituents);

Reactive Transport Modeling: Applications in Subsurface Energy and Environmental Problems, First Edition. Edited by Yitian Xiao, Fiona Whitaker, Tianfu Xu and Carl Steefel.

- the plant model (growth, decay, decomposition, nutrient uptake, root oxygen release, etc);
- the clogging model (the transport and deposition of suspended particulate matter, and bacterial and plant growth that may reduce the hydraulic capacity/conductivity of the filter medium).

Different types of CWs require different models to describe water flow. No free water level is visible in subsurface flow (SSF) CWs, and water flows, either horizontally or vertically, through the porous filter media. Horizontal flow (HF) systems can be simulated when only saturated water flow conditions are considered. For modeling vertical flow (VF) CWs with intermittent loading, transient variably-saturated flow models are required. Due to the intermittent loading, these systems are highly dynamic, adding to the complexity needed to model the overall system. Models applicable to VF CWs use either the Richards equation or various simplified approaches to describe variably-saturated flow (Langergraber, 2008).

Wastewaters contain particulate and solute compounds that are transported with the flowing water. Transport equations generally consider convective–dispersive transport in the liquid phase, diffusion in the gaseous phase, as well as adsorption and desorption processes between the solid and liquid phases.

Biokinetic models describe the transformation and degradation processes of the pollutants. The complexity of biokinetic models ranges from considering a single process affecting the concentration of one compound to multiple processes affecting multiple compounds. The reaction rates are often assumed to be constant, that is, independent of environmental conditions. However, reaction rates are dependent on a number of environmental conditions (e.g. concentrations of oxygen, substrate, nutrients). These dependencies are often modeled with Monod-type equations.

Plants are an essential part of wetland treatment systems, and thus plant-related processes have to be included in wetland models. Root growth influences the water flow pattern in the subsurface, and via evapotranspiration the water balance. During growth and decay, plants take up nutrients and release organic matter and nutrients, respectively. Additionally, some plants release substances via roots (e.g. oxygen and/or specific organic substances). Plant models describe uptake and release of substances either associated with water uptake or as a process dependent on concentration gradients.

Clogging models need to be able to describe (1) the transport and deposition of suspended particulate matter, and (2) the deposition of particulate matter, bacterial and plant growth that may reduce the hydraulic capacity/conductivity of the filter medium. This is important for simulations of the long-term CW performance and predictions of potential failure due to clogging (Langergraber and Morvannou, 2014).

During the last two decades a couple of mechanistic models have been developed for simulating CWs (Langergraber, 2008, Langergraber et al., 2009a; Kumar and Zhao, 2011; Meyer et al., 2015; Samsó et al., 2015b). Recent developments, especially towards implementation of the CWM1 biokinetic model (Langergraber et al., 2009b), include the works of Langergraber and Šimůnek (2012), Samsó and Garcia (2013), and Mburu et al. (2012). Table 9.1 compares three tools with respect to the considered submodels required for a wetland model.

In this chapter, we briefly describe version 2 of the HYDRUS Wetland module (Langergraber and Šimůnek, 2012) and discuss existing experience using wetland

Table 9.1 Comparison of recent simulation tools for constructed wetlands.

Simulation tool	HYDRUS Wetland module	BIO_PORE	AQUASIM
Reference	Langergraber and Šimůnek (2012)	Samsó and Garcia (2013)	Mburu et al. (2012)
Flow model	Richards equation (variably saturated flow)	Variable water table (saturated flow)	No flow considered
Transport model	Advection, dispersion, adsorption	Advection, dispersion, adsorption	No transport model
Biokinetic model	CW2D + CWM1	CWM1	CWM1
Influence of plants	Evapotranspiration, uptake and release of substances	Evapotranspiration, uptake and release of substances	Evapotranspiration, uptake and release of substances
Clogging model	Not considered	Included	Not considered

models in general and the HYDRUS Wetland module in particular. We further describe remaining challenges in using these tools and summarize needs for further development and research.

9.2 The HYDRUS Wetland Module

The HYDRUS software numerically solves the Richards equation for saturated/unsaturated water flow and the convection–dispersion equation for heat and solute transport. The flow equation incorporates a sink term to account for water uptake by plant roots. The solute transport equations consider convective–dispersive transport in the liquid phase, diffusion in the gaseous phase, as well as nonlinear nonequilibrium reactions between the solid and liquid phases (Šimůnek et al., 2008, 2011).

Version 2 of the HYDRUS wetland module (Langergraber and Šimůnek, 2012) includes two biokinetic model formulations: (1) the CW2D (Langergraber and Šimůnek, 2005), and (2) the CWM1 (Constructed Wetland Model 1) biokinetic models (Langergraber et al., 2009b). In CW2D, aerobic and anoxic transformation and degradation processes for organic matter, nitrogen and phosphorus are taken into account, whereas in CWM1, aerobic, anoxic and anaerobic processes for organic matter, nitrogen and sulfur are considered. CWM1 has been developed with the main goal of providing a widely accepted model formulation for biochemical transformation and degradation processes in SSF CWs. Table 9.2 summarizes processes and components described by, and applications of, the biokinetic models CW2D and CWM1, which are implemented in the HYDRUS Wetland module.

Both CW2D and CWM1 have been developed to describe processes in constructed wetlands treating domestic wastewater. A number of applications of the HYDRUS wetland module shows that a good match between measured data and simulation results can be achieved (e.g. Langergraber, 2003, 2007; Langergraber et al., 2007). In addition to

Table 9.2 Processes and components described by (number of components/processes in brackets), and applications of, the biokinetic models CW2D and CWM1 (adapted from Langergraber and Šimůnek, 2012).

Biokinetic model	CW2D	CWM1
Processes	Aerobic and anoxic (9)	Aerobic, anoxic, and anaerobic (17)
Components	Oxygen, organic matter, nitrogen, and phosphorus (12)	Oxygen, organic matter, nitrogen, and sulfur (16)
Type of CW	VF CWs Low-loaded HF beds	VF and HF CWs

applications involving treatment of municipal wastewater in CWs, the HYDRUS Wetland module has been also used to model:

- CWs treating combined sewer overflow (Dittmer et al., 2005; Henrichs et al. 2007, 2009; Meyer, 2011)
- CWs treating effluents of the wastewater treatment plant for irrigation purposes (Toscano et al., 2009; Pálfy et al., 2015a)
- CWs treating artificial wastewater (e.g. Pálfy and Langergraber, 2014; Rizzo et al., 2014)
- CWs treating greywater (Karlsson et al., 2015)
- Runoff from agricultural sites and the effects of streamside management zones (Smethurst et al., 2014).

Besides the Wetland module, the HYDRUS software also includes the HP1/2/3 multi-component solute transport modules, the colloid-facilitated solute transport C-Ride module, a module for fumigants, and the major ion UnsatChem module. All of these modules simulate water flow and solute/heat transport processes in two-dimensional transport domains and are supported by the HYDRUS (2D/3D) graphical user interface. Many processes of these specialized modules are also available as part of the public domain HYDRUS-1D software (Šimůnek et al., 2013).

9.3 The CW2D and CWM1 Biokinetic Models

In this section, the CW2D and CWM1 biokinetic models (i.e., the components and processes defined in the two models) are presented in detail. The information is derived from the original papers of Langergraber and Šimůnek (2005) and Langergraber et al. (2009b), respectively.

Table 9.3 compares the components defined in the CW2D and CWM1 model formulations. As described above, both biokinetic models consider processes affecting organic matter and nitrogen. Additionally, CW2D considers processes affecting phosphorus, whereas CWM1 considers processes affecting sulfur. All components except bacteria are assumed to be soluble (including the particulate Chemical Oxygen Demand (COD) fraction) and bacteria are immobile. Organic nitrogen (in CW2D and CWM1) and organic phosphorus (in CW2D) are modeled as part of the COD. Since wastewater

Table 9.3 Comparison of CW2D and CWM1 components in the HYDRUS implementation.

CW2D (Langergraber and Šimůnek, 2005) Organic matter, nitrogen, phosphorus	**CWM1 (Langergraber et al., 2009b)** Organic matter, nitrogen, sulfur
CW2D components 1) SO: Dissolved oxygen, O_2 2) CR: Readily biodegradable soluble COD 3) CS: Slowly biodegradable soluble COD 4) CI: Inert soluble COD 5) XH: Heterotrophic bacteria 6) XANs: Autotrophic ammonia oxidizing bacteria (Nitrosomonas spp.) 7) XANb: Autotrophic nitrite oxidizing bacteria (Nitrobacter spp.) 8) NH4N: Ammonium and ammonia nitrogen 9) NO2N: Nitrite nitrogen 10) NO3N: Nitrate nitrogen 11) N2: Elemental nitrogen 12) PO4P: Phosphate phosphorus *Additional component (in the HYDRUS implementation)* 13) Non-reactive tracer Nitrification is modeled as a two-step process	*Soluble components* 1) SO: Dissolved oxygen, O_2 2) SF: Fermentable, readily biodegradable soluble COD 3) SA: Fermentation products as acetate 4) SI: Inert soluble COD 5) SNH: Ammonium and ammonia nitrogen 6) SNO: Nitrate and nitrite nitrogen 7) SSO4: Sulfate sulfur 8) SH2S: Dihydrogensulfide sulfur *Particulate components* 9) XS: Slowly biodegradable particulate COD 10) XI: Inert particulate COD 11) XH: Heterotrophic bacteria 12) XA: Autotrophic nitrifying bacteria 13) XFB: Fermenting bacteria 14) XAMB: Acetotrophic methanogenic bacteria 15) XASRB: Acetotrophic sulfate reducing bacteria 16) XSOB: Sulfide oxidizing bacteria *Additional component (in the HYDRUS implementation)* 17) Non-reactive tracer

Table 9.4 Definitions of CW2D and CWM1 components in the liquid and solid phases (Langergraber and Šimůnek, 2011).

Component	**1**	**2**	**3**	**4**	**5**	**6**	**7**	**8**	**9**	**10**	**11**	**12**	**13**	**14**	**15**	**16**	**17**
CW2D	L	L+S	L+S	L+S	S	S	S	L+S	L	L	L	L+S	L+S	–	–	–	–
CWM1	L	L+S	L+S	L+S	L+S	L	L	L	L+S	L+S	S	S	S	S	S	S	L+S

L, defined in the liquid phase only; S, defined in the solid phase only; L + S, defined in both liquid and solid phases.

constituents considered in the CW2D and CWM1 biokinetic models are different, there is no direct conversion between two model components.

Table 9.4 summarizes in what phase (i.e. liquid and/or solid) the CW2D and CWM1 components are defined in the HYDRUS Wetland module. For components defined in both phases (L + S), adsorption and desorption processes can be considered. As mentioned above, suspended particulate organic matter compounds (XS and XI in CWM1)

are considered as solute compounds. Note that the number of components in Table 9.4 is increased by one compared with that given in Table 9.2 for both CW2D and CWM1. In both models, a non-reactive tracer that is independent of other components, and that can be used to derive the hydraulic retention time, is added in the HYDRUS wetland module. This non-reactive tracer is defined in both liquid and solid phases (Langergraber and Šimůnek, 2011).

Table 9.5 compares the processes defined in the CW2D and CWM1 model formulations. Only aerobic and anoxic processes are defined in CW2D. Two main types of bacteria, heterotrophic and autotrophic bacteria, are considered. One special feature of CW2D is that nitrification is modeled as a two-step process, from ammonia via nitrite to nitrate. Since anaerobic processes are additionally defined in CWM1, six different types of bacteria need to be considered in this model. In addition to heterotrophic and

Table 9.5 Comparison of CW2D and CWM1 processes (Langergraber and Šimůnek, 2011).

CW2D (Langergraber and Šimůnek, 2005)	**CWM1 (Langergraber et al., 2009b)**
Heterotrophic bacteria: 1) Hydrolysis: conversion of CS into CR 2) Aerobic growth of XH on CR (mineralization of organic matter) 3) Anoxic growth of XH on CR (denitrification on NO2N) 4) Anoxic growth of XH on CR (denitrification on NO3N) 5) Lysis of XH *Autotrophic bacteria:* 6) Aerobic growth of XANs on SNH (ammonium oxidation) 7) Lysis of XANs 8) Aerobic growth of XANb on SNH (nitrite oxidation) 9) Lysis of XANb	*Heterotrophic bacteria:* 1) Hydrolysis: conversion of XS into SF 2) Aerobic growth of XH on SF (mineralization of organic matter) 3) Aerobic growth of XH on SA (mineralization of organic matter) 4) Anoxic growth of XH on SF (denitrification) 5) Anoxic growth of XH on SA (denitrification) 6) Lysis of XH *Autotrophic bacteria:* 7) Aerobic growth of XA on SNH (nitrification) 8) Lysis of XA *Fermenting bacteria:* 9) Growth of XFB (fermentation) 10) Lysis of XFB *Acetotrophic methanogenic bacteria*: 11) Growth of XAMB: Anaerobic growth of acetotrophic, methanogenic bacteria XAMB on acetate SA 12) Lysis of XAMB *Acetotrophic sulfate reducing bacteria*: 13) Growth of XASRB: Anaerobic growth of acetotrophic, sulfate reducing bacteria 14) Lysis of XASRB *Sulfide oxidizing bacteria*: 15) Aerobic growth of XSOB on SH2S: The opposite process to 13, the oxidation of SH2S to SSO4 16) Anoxic growth of XSOB on SH2S: Similar to process 15 but under anoxic conditions 17) Lysis of XSOB

autotrophic bacteria, fermenting, acetotrophic methanogenic, acetotrophic sulfate reducing, and sulfide oxidizing bacteria are also considered, in order to account for the main anaerobic processes.

9.3.1 CW2D Biokinetic Model

9.3.1.1 Stoichiometric Matrix and Reaction Rates

Table 9.6 and Table 9.7 show stoichiometric coefficients for ammonium nitrogen and inorganic phosphorus, respectively. Table 9.8 shows the stoichiometric matrix of reactions in CW2D, whereas Table 9.9 shows the reaction rates.

9.3.1.2 Model Parameters

Table 9.10 shows the kinetic parameters, and Table 9.11 the temperature dependences, stoichiometric parameters, composition parameters and parameters describing oxygen transfer for the CW2D biokinetic model, as described in Langergraber and Šimůnek (2005).

Table 9.6 Stoichiometric coefficients for ammonium nitrogen (Langergraber and Šimůnek, 2011; see Table 9.11 for definitions of the composition and stoichiometric parameters).

$\nu_{1,N}$ =	$i_{N,CS} - (1 - f_{Hyd,CI}).i_{N,CR} - f_{Hyd,CI}.i_{N,CI}$
$\nu_{2,N}$ =	$1/Y_H.i_{N,CR} - i_{N,BM}$
$\nu_{3,N}$ =	$1/Y_H.i_{N,CR} - i_{N,BM}$
$\nu_{4,N}$ =	$1/Y_H.i_{N,CR} - i_{N,BM}$
$\nu_{5,N}$ =	$i_{N,BM} - (1 - f_{BM,CR} - f_{BM,CI}).i_{N,CS} - f_{BM,CR}.i_{N,CR} - f_{BM,CI}.i_{N,CI}$
$\nu_{6,N}$ =	$-1/Y_{ANs} - i_{N,BM}$
$\nu_{7,N}$ =	$i_{N,BM} - (1 - f_{BM,CR} - f_{BM,CI}).i_{N,CS} - f_{BM,CR}.i_{N,CR} - f_{BM,CI}.i_{N,CI}$
$\nu_{8,N}$ =	$-i_{N,BM}$
$\nu_{9,N}$ =	$i_{N,BM} - (1 - f_{BM,CR} - f_{BM,CI}).i_{N,CS} - f_{BM,CR}.i_{N,CR} - f_{BM,CI}.i_{N,CI}$

Table 9.7 Stoichiometric coefficients for inorganic phosphorus (Langergraber and Šimůnek, 2011; see Table 9.11 for definitions of the composition and stoichiometric parameters).

$\nu_{1,P}$ =	$i_{P,CS} - (1 - f_{Hyd,CI}).i_{P,CR} - f_{Hyd,CI}.i_{P,CI}$
$\nu_{2,P}$ =	$1/Y_H.i_{P,CR} - i_{P,BM}$
$\nu_{3,P}$ =	$1/Y_H.i_{P,CR} - i_{P,BM}$
$\nu_{4,P}$ =	$1/Y_H.i_{P,CR} - i_{P,BM}$
$\nu_{5,P}$ =	$i_{P,BM} - (1 - f_{BM,CR} - f_{BM,CI}).i_{P,CS} - f_{BM,CR}.i_{P,CR} - f_{BM,CI}.i_{P,CI}$
$\nu_{6,P}$ =	$-i_{P,BM}$
$\nu_{7,P}$ =	$i_{P,BM} - (1 - f_{BM,CR} - f_{BM,CI}).i_{P,CS} - f_{BM,CR}.i_{P,CR} - f_{BM,CI}.i_{P,CI}$
$\nu_{8,P}$ =	$-i_{P,BM}$
$\nu_{9,P}$ =	$i_{P,BM} - (1 - f_{BM,CR} - f_{BM,CI}).i_{P,CS} - f_{BM,CR}.i_{P,CR} - f_{BM,CI}.i_{P,CI}$

Table 9.8 CW2D stoichiometric matrix (Langergraber and Šimůnek, 2005; see Table 9.11 for definitions of the stoichiometric coefficients).

	i →		1	2	3	4	5	6	7	8	9	10	11	12
j	**Process**	**Component**	**O2**	**CR**	**CS**	**CI**	**XH**	**XANs**	**XANb**	**NH4N**	**NO2N**	**NO3N**	**N2N**	**IP**
↓		expressed as →	O_2	COD	COD	COD	COD	COD	COD	N	N	N	N	P
1	Hydrolysis			$1-f_{\mathrm{Hyd,CR}}$	−1	$1-f_{\mathrm{Hyd,CI}}$				$\nu_{1,N}$				$\nu_{1,P}$
2	Aerobic growth of heterotrophs on readily biodegradable COD		$1-\frac{1}{Y_H}$	$-1/Y_{\mathrm{H}}$			1			$\nu_{2,N}$				$\nu_{2,P}$
3	NO_3-growth of heterotrophs on readily biodegradable COD			$-1/Y_{\mathrm{H}}$			1			$\nu_{3,N}$		$-\frac{1-Y_H}{2.86\cdot Y_H}$	$\frac{1-Y_H}{2.86\cdot Y_H}$	$\nu_{3,P}$
4	NO_2-growth of heterotrophs on readily biodegradable COD			$-1/Y_{\mathrm{H}}$			1			$\nu_{4,N}$	$-\frac{1-Y_H}{1.71\cdot Y_H}$		$\frac{1-Y_H}{1.71\cdot Y_H}$	$\nu_{4,P}$
5	Lysis of heterotrophs			$f_{\mathrm{BM,CR}}$	ν_{Lysis}	$f_{\mathrm{BM,CI}}$	−1			$\nu_{5,N}$				$\nu_{5,P}$
6	Aerobic growth of *Nitrosomonas* on NH_4		$-\frac{3.43-Y_A}{Y_A}$					1		$i_{\mathrm{N,BM}}-1/Y_{\mathrm{ANs}}$	$1/Y_{\mathrm{ANs}}$			$\nu_{6,P}$
7	Lysis of *Nitrosomonas*			$f_{\mathrm{BM,CR}}$	ν_{Lysis}	$f_{\mathrm{BM,CI}}$		−1		$\nu_{7,N}$				$\nu_{7,P}$
8	Aerobic growth of *Nitrobacter* on NO_2		$-\frac{1.14-Y_A}{Y_A}$						1	$\nu_{8,N}$	$-1/Y_{\mathrm{ANb}}$	$1/Y_{\mathrm{ANb}}$		$\nu_{8,P}$
9	Lysis of *Nitrobacter*			$f_{\mathrm{BM,CR}}$	ν_{Lysis}	$f_{\mathrm{BM,CI}}$			−1	$\nu_{9,N}$				$\nu_{9,P}$

$\nu_{\mathrm{Lysis}} = 1\text{-}f_{BM,CR}\text{-}f_{BM,CI}$

Table 9.9 Reaction rates in CW2D (Langergraber and Šimůnek, 2005; see Table 9.10 for definitions of rate coefficients).

R	Process/reaction rate rc_j
	Heterotrophic organisms
1)	Hydrolysis $K_h \cdot \frac{c_{CS}/c_{XH}}{K_X + c_{CS}/c_{XH}} \cdot c_{XH}$
2)	Aerobic growth of heterotrophs on readily biodegradable COD $\mu_H \cdot \frac{c_{O2}}{K_{Het,O2} + c_{O2}} \cdot \frac{c_{CR}}{K_{Het,CR} + c_{CR}} \cdot f_{N,Het} \cdot c_{XH}$
3)	NO_3-growth of heterotrophs on readily biodegradable COD $\mu_{DN} \cdot \frac{K_{DN,O2}}{K_{DN,O2} + c_{O2}} \cdot \frac{c_{NO3}}{K_{DN,NO3} + c_{NO3}} \cdot \frac{K_{DN,NO2}}{K_{DN,NO2} + c_{NO2}} \cdot \frac{c_{CR}}{K_{DN,CR} + c_{CR}} \cdot f_{N,DN} \cdot c_{XH}$
4)	NO_2-growth of heterotrophs on readily biodegradable COD $\mu_{DN} \cdot \frac{K_{DN,O2}}{K_{DN,O2} + c_{O2}} \cdot \frac{c_{NO2}}{K_{DN,NO2} + c_{NO2}} \cdot \frac{c_{CR}}{K_{DN,CR} + c_{CR}} \cdot f_{N,DN} \cdot c_{XH}$
5)	Lysis of heterotrophs $b_H \cdot c_{XH}$
	Autotrophic organisms 1 – Nitrosomonas
6)	Aerobic growth of *Nitrosomonas* on NH_4 $\mu_{ANs} \cdot \frac{c_{O2}}{K_{ANs,O2} + c_{O2}} \cdot \frac{c_{NH4}}{K_{ANs,NH4} + c_{NH4}} \cdot \frac{c_{IP}}{K_{ANs,IP} + c_{IP}} \cdot c_{XANs}$
7)	Lysis of *Nitrosomonas* $b_{HANs} \cdot c_{XANs}$
	Autotrophic organisms 2 – Nitrobacter
8)	Aerobic growth of *Nitrobacter* on NO_2 $\mu_{ANb} \cdot \frac{c_{O2}}{K_{ANb,O2} + c_{O2}} \cdot \frac{c_{NO2}}{K_{ANb,NO2} + c_{NO2}} \cdot f_{N,ANb} \cdot c_{XANb}$
9)	Lysis of *Nitrobacter* $b_{HANb} \cdot c_{XANb}$
	Conversion of solid and liquid phase concentrations $c_{XY} = \frac{\rho}{\theta} \cdot s_{XY}$, where $Y = \mathrm{H},\ \mathrm{ANs},\ \mathrm{ANb}$
	Factor for nutrients $f_{N,x} = \frac{c_{NH4}}{K_{x,NH4} + c_{NH4}} \cdot \frac{c_{IP}}{K_{x,IP} + c_{IP}}$, where $x = \mathrm{Het},\ \mathrm{DN},\ \mathrm{ANb}$

Table 9.10 Kinetic parameters in the CW2D biokinetic model (Langergraber and Šimůnek, 2005).

Parameter	Description [unit]	Value
Hydrolysis		For 20 °C (10 °C)
K_h	Hydrolysis rate constant [1/d]	3 (2)
K_X	Saturation/inhibition coefficient for hydrolysis [g COD_{CS}/g COD_{BM}]	0.1 (0.22)*
Heterotrophic bacteria (aerobic growth)		
μ_H	Maximum aerobic growth rate on CR [1/d]	6 (3)
b_H	Rate constant for lysis [1/d]	0.4 (0.2)
$K_{het,O2}$	Saturation/inhibition coefficient for S_O [mg O_2/l]	0.2
$K_{het,CR}$	Saturation/inhibition coefficient for substrate [mg COD_{CR}/l]	2
$K_{het,NH4N}$	Saturation/inhibition coefficient for NH_4 (nutrient) [mg N/l]	0.05
$K_{het,IP}$	Saturation/inhibition coefficient for P [mg N/l]	0.01
Heterotrophic bacteria (denitrification)		
μ_{DN}	Maximum aerobic growth rate on CR [1/d]	4.8 (2.4)
$K_{DN,O2}$	Saturation/inhibition coefficient for S_O [mg O_2/l]	0.2
$K_{DN,NO3N}$	Saturation/inhibition coefficient for NO_3 [mg N/l]	0.5
$K_{DN,NO2N}$	Saturation/inhibition coefficient for NO_2 [mg N/l]	0.5
$K_{DN,CR}$	Saturation/inhibition coefficient for substrate [mg COD_{CR}/l]	4
$K_{DN,NH4N}$	Saturation/inhibition coefficient for NH_4 (nutrient) [mg N/l]	0.05
$K_{DN,IP}$	Saturation/inhibition coefficient for P [mg N/l]	0.01
Ammonia oxidizing bacteria (Nitrosomonas spp.)		
μ_{ANs}	Maximum aerobic growth rate on S_{NH} [1/d]	0.9 (0.3)
b_{ANs}	Rate constant for lysis [1/d]	0.15 (0.05)
$K_{ANs,O2}$	Saturation/inhibition coefficient for S_O [mg O_2/l]	1
$K_{ANs,NH4N}$	Saturation/inhibition coefficient for NH_4 [mg N/l]	0.5 (5.5)*
$K_{ANs,IP}$	Saturation/inhibition coefficient for P [mg N/l]	0.01
Nitrite oxidizing bacteria (Nitrobacter spp.)		
μ_{ANb}	Maximum aerobic growth rate on S_{NH} [1/d]	1 (0.35)
b_{ANb}	Rate constant for lysis [1/d]	0.15 (0.05)
$K_{ANb,O2}$	Saturation/inhibition coefficient for S_O [mg O_2/l]	0.1
$K_{ANb,NO2N}$	Saturation/inhibition coefficient for NO_2 [mg N/l]	0.1
$K_{ANb,NH4N}$	Saturation/inhibition coefficient for NH_4 (nutrient) [mg N/l]	0.05
$K_{ANb,IP}$	Saturation/inhibition coefficient for P [mg N/l]	0.01

*Langergraber (2007).

Table 9.11 Temperature dependences, stoichiometric parameters, composition parameters and parameters describing oxygen transfer in the CW2D biokinetic model (Langergraber and Šimůnek, 2005).

Parameter	Description [unit]	Value
Temperature dependencies (activation energy [J/mol] for Arrhenius equation)		
Tdep_het	Activation energy for processes caused by XH [J/mol]	47,800
Tdep_aut	Activation energy for processes caused by XA [J/mol]	69,000
Tdep_Kh	Activation energy hydrolyses [J/mol]	28,000
Tdep_KX	Activation energy factor KX for hydrolyses [J/mol]	−53,000*
Tdep_KNHA	Activation energy for factor KNHA for nitrification [J/mol]	−160,000*
Stoichiometric parameters		
$f_{Hyd,CI}$	Production of CI in hydrolysis	0.0
$f_{BM,CR}$	Fraction of CR generated in biomass lysis	0.1
$f_{BM,CI}$	Fraction of CI generated in biomass lysis	0.02
Y_{Het}	Yield coefficient for XH	0.63
Y_{ANs}	Yield coefficient for XANs	0.24
Y_{ANb}	Yield coefficient for XANb	0.24
Composition parameters		
$i_{N,CR}$	N content of CR [g N/g COD_{CR}]	0.03
$i_{N,CS}$	N content of CS [g N/g COD_{CS}]	0.04
$i_{N,CI}$	N content of CI [g N/g COD_{CI}]	0.01
$i_{N,BM}$	N content of biomass [g N/g COD_{BM}]	0.07
$i_{P,CR}$	P content of CR [g P/g COD_{CR}]	0.01
$i_{P,CS}$	P content of CS [g P/g COD_{CS}]	0.01
$i_{P,CI}$	P content of CI [g P/g COD_{CI}]	0.01
$i_{P,BM}$	P content of biomass [g P/g COD_{BM}]	0.02
Oxygen		
cO2_sat_20	Saturation concentration of oxygen [g/m^3]	9.18
Tdep_cO2_sat	Activation energy for saturation concentration of oxygen [J/mol]	−15,000
rate_O2	Re-aeration rate [1/d]	240

*Langergraber (2007).

9.3.2 CWM1 Biokinetic Model

9.3.2.1 Stoichiometric Matrix and Reaction Rates

Table 9.12 shows the stoichiometric matrix of reactions in CWM1, Table 9.13 the stoichiometric coefficients for ammonium nitrogen, and Table 9.14 the reaction rates.

Table 9.12 CWM1 stoichiometric matrix (Langergraber et al., 2009b; see Table 9.17 for definitions of the stoichiometric coefficients).

	i →		1	2	3	4	5	6	7	8	9	10	11	12	13	14	15	16
j	**Process**	**Component**	**SO**	**SF**	**SA**	**SI**	**SNH**	**SNO**	**SSO4**	**SH2S**	**XS**	**XI**	**XH**	**XA**	**XFB**	**XAMB**	**XASRB**	**XSOB**
↓		expressed as →	O_2	COD	COD	COD	N	N	S	S	COD	COD	COD	COD	COD	COD	COD	COD
1	Hydrolysis			$1-f_{Hyd,SI}$		$f_{Hyd,SI}$	$\nu_{1,5}$				-1							
2	Aerobic growth of X_H on S_F		$1-\frac{1}{Y_H}$	$-1/Y_H$			$\nu_{2,5}$						1					
3	Anoxic growth of X_H on S_F			$-1/Y_H$			$\nu_{3,5}$	$-\frac{1-Y_H}{2.86\cdot Y_H}$					1					
4	Aerobic growth of X_H on S_A		$1-\frac{1}{Y_H}$		$-1/Y_H$		$\nu_{4,5}$						1					
5	Anoxic growth of X_H on S_A				$-1/Y_H$		$\nu_{5,5}$	$-\frac{1-Y_H}{2.86\cdot Y_H}$					1					
6	Lysis of X_H			$f_{BM,SF}$			$\nu_{6,5}$				ν_{Lysis}	$f_{BM,XI}$	-1					
7	Aerobic growth of X_A on S_{NH}		$-\frac{4.57-Y_A}{Y_A}$				$-i_{N,BM}-\frac{1}{Y_A}$	$1/Y_A$						1				
8	Lysis of X_A			$f_{BM,SF}$			$\nu_{8,5}$				ν_{Lysis}	$f_{BM,XI}$		-1				
9	Growth of X_{FB}			$-1/Y_{FB}$	$\frac{1-Y_{FB}}{Y_{FB}}$		$\nu_{9,5}$								1			
10	Lysis of X_{FB}			$f_{BM,SF}$			$\nu_{10,5}$				ν_{Lysis}	$f_{BM,XI}$			-1			

11	Growth of X_{AMB}			$-1/Y_{AMB}$	$\nu_{11,5}$							1		
12	Lysis of X_{AMB}		$f_{BM,SF}$		$\nu_{12,5}$				ν_{Lysis}	$f_{BM,XI}$		-1		
13	Growth of X_{ASRB}			$-1/Y_{ASRB}$	$\nu_{13,5}$		$-\frac{1-Y_{ASRB}}{2\cdot Y_{ASRB}}$	$\frac{1-Y_{ASRB}}{2\cdot Y_{ASRB}}$					1	
14	Lysis of X_{ASRB}		$f_{BM,SF}$		$\nu_{14,5}$				ν_{Lysis}	$f_{BM,XI}$			-1	
15	Aerobic growth of X_{SOB} on S_{H2S}	$-\frac{2-Y_{SOB}}{Y_{SOB}}$			$\nu_{15,5}$		$1/Y_{SOB}$	$-1/Y_{SOB}$						1
16	Anoxic growth of X_{SOB} on S_{H2S}				$\nu_{16,5}$	$-\frac{1-Y_{SOB}}{0.875\cdot Y_{SOB}}$	$1/Y_{SOB}$	$-1/Y_{SOB}$						1
17	Lysis of X_{SOB}		$f_{BM,SF}$		$\nu_{17,5}$				ν_{Lysis}	$f_{BM,XI}$				-1

$\nu_{Lysis} = 1 - f_{BM,SF} - f_{BM,XI}$

Table 9.13 Stoichiometric coefficients for ammonia nitrogen (see Table 9.17 for definitions of the composition and stoichiometric parameters).

$\nu_{1,5} =$	$i_{N,XS} - (1 - f_{HYD,SI}) * i_{N,SF} - f_{HYD,SI} * i_{N,SI}$
$\nu_{2,5} = \nu_{3,5} =$	$i_{N,SF}/Y_H - i_{N,BM}$
$\nu_{4,5} = \nu_{5,5} = \nu_{11,5} = \nu_{13,5} = \nu_{15,5} = \nu_{16,5} =$	$-i_{N,BM}$
$\nu_{6,5} = \nu_{8,5} = \nu_{10,5} = \nu_{12,5} = \nu_{14,5} = \nu_{17,5} =$	$i_{N,BM} - f_{BM,SF} * i_{N,SF} - (1 - f_{BM,SF} - f_{BM,XI}) * i_{N,XS} - f_{BM,XI} * i_{N,XI}$
$\nu_{7,5} =$	$-i_{N,BM} - \frac{1}{Y_A}$
$\nu_{9,5} =$	$i_{N,SF}/Y_{FB} - i_{N,BM}$

9.3.2.2 Model Parameters

Table 9.15 shows the kinetic parameters in the CWM1 biokinetic model; Table 9.16 temperature dependences, stoichiometric parameters, composition parameters and parameters describing oxygen transfer as described in Langergraber et al. (2009b).

9.4 Simulation Results for Vertical Flow Constructed Wetlands Treating Domestic Wastewater

This section shows typical simulation results for VF CWs. As described by Langergraber (2008), VF pilot-scale CWs (Figure 9.1) have been operated in the technical laboratory hall of the Institute of Sanitary Engineering at BOKU University in Vienna, Austria. The systems had a surface area of 1 m^2 and were loaded four times per day with mechanically pre-treated municipal wastewater. The 60 cm main layer consisted of sand with a grain size of 0.06–4 mm (d_{10} = 0.2 mm; d_{60} = 0.8 mm). The intermediate layer (gravel 4–8 mm) prevents fine particles from being washed out into the drainage layer (gravel 16–32 mm).

For the numerical simulations, only the main layer was considered. The transport domain (i.e. a vertical cross-section of the main layer) was discretized into 11 columns and 40 rows. This resulted in a two-dimensional finite element mesh consisting of 440 nodes and 780 finite elements. An atmospheric boundary condition is assigned to the top of the system, a constant pressure head boundary condition with constant head of −2 cm (Langergraber, 2008).

Table 9.17 shows three parameter sets of the van Genuchten-Mualem model (van Genuchten, 1980) of the soil hydraulic properties used in simulations of water flow. The "HYDRUS parameter set for 'Sand'" uses default soil hydraulic properties for sand provided by HYDRUS, the '*Measured K_s and porosity*' parameter set measured values of porosity and saturated hydraulic conductivity K_s, and the default residual water content and shape parameters for sand. The third parameter set was obtained by inverse simulation. Measured effluent flow rates were used to estimate the soil hydraulic parameters (i.e. residual water content and shape parameters) using the inverse simulation routine provided by HYDRUS (Šimůnek et al., 2011). Measured values of porosity and K_s were kept constant. Figure 9.2 compares the measured and simulated effluent flow rates using these three parameter sets. The simulated effluent flow rates are rather constant when using the default parameter set for sand due to the low K_s value. When using

Table 9.14 Reaction rates in CWM1 part 1 (Langergraber et al., 2009b; see Tables 9.16 and 9.17 for definitions of rate coefficients).

R	Process/reaction rate rc_j
	Heterotrophic organisms
1)	Hydrolysis $k_h * \left[\frac{X_S / (X_H + X_{FB})}{K_X + (X_S / (X_H + X_{FB}))} \right] * (X_H + \eta_h * X_{FB})$
2)	Aerobic growth of XH on SF (mineralization) $\mu_H * \left(\frac{S_F}{K_{SF} + S_F} \right) * \left(\frac{S_F}{S_F + S_A} \right) * \left(\frac{S_O}{K_{OH} + S_o} \right) * \left(\frac{S_{NH}}{K_{NHH} + S_{NH}} \right) * \left(\frac{K_{H2SH}}{K_{H2SH} + S_{H2S^*}} \right) * X_H$
3)	Aerobic growth of XH on SA (mineralization) $\eta_g * \mu_H * \left(\frac{S_F}{K_{SF} + S_F} \right) * \left(\frac{S_F}{S_F + S_A} \right) * \left(\frac{K_{OH}}{K_{OH} + S_o} \right) * \left(\frac{S_{NO}}{K_{NOH} + S_{NO}} \right) * \left(\frac{S_{NH}}{K_{NHH} + S_{NH}} \right) * \left(\frac{K_{H2SH}}{K_{H2SH} + S_{H2S^*}} \right) * X_H$
4)	Anoxic growth of XH on SF (denitrification) $\mu_H * \left(\frac{S_A}{K_{SA} + S_A} \right) * \left(\frac{S_A}{S_F + S_A} \right) * \left(\frac{S_O}{K_{OH} + S_o} \right) * \left(\frac{S_{NH}}{K_{NHH} + S_{NH}} \right) * \left(\frac{K_{H2SH}}{K_{H2SH} + S_{H2S^*}} \right) * X_H$
5)	Anoxic growth of XH on SA (denitrification) $\eta_g * \mu_H * \left(\frac{S_A}{K_{SA} + S_A} \right) * \left(\frac{S_A}{S_F + S_A} \right) * \left(\frac{K_{OH}}{K_{OH} + S_o} \right) * \left(\frac{S_{NO}}{K_{NOH} + S_{NO}} \right) * \left(\frac{S_{NH}}{K_{NHH} + S_{NH}} \right) * \left(\frac{K_{H2SH}}{K_{H2SH} + S_{H2S^*}} \right) * X_H$
6)	Lysis of XH $b_H * X_H$
	Autotrophic bacteria
7)	Aerobic growth of XA on SNH (nitrification) $\mu_A * \left(\frac{S_{NH}}{K_{NHA} + S_{NH}} \right) * \left(\frac{S_O}{K_{OA} + S_o} \right) * \left(\frac{K_{H2SA}}{K_{H2SA} + S_{H2S^*}} \right) * X_A$
8)	Lysis of XA $b_A * X_A$
	Fermenting bacteria
9)	Growth of XFB (fermentation) $\mu_{FB} * \left(\frac{S_F}{K_{SFB} + S_F} \right) * \left(\frac{K_{H2SFB}}{K_{H2SFB} + S_{H2S^*}} \right) * \left(\frac{K_{OFB}}{K_{OFB} + S_O} \right) * \left(\frac{K_{NOFB}}{K_{NOFB} + S_{NO}} \right) * \left(\frac{S_{NH}}{K_{NHFB} + S_{NH}} \right) * X_{FB}$

(*Continued*)

Table 9.14 (Continued)

R	Process/reaction rate rc_j
	10) Lysis of XFB
	$b_{FB} * X_{FB}$
	Acetotrophic methanogenic bacteria
	11) Growth of XAMB
	$\mu_{AMB} * \left(\frac{S_A}{K_{SAMB} + S_A}\right) * \left(\frac{K_{H2SAMB}}{K_{H2SAMB} + S_{H2S^*}}\right) * \left(\frac{K_{OAMB}}{K_{OAMB} + S_O}\right) * \left(\frac{K_{NOAMB}}{K_{NOAMB} + S_{NO}}\right) * \left(\frac{S_{NH}}{K_{NHAMB} + S_{NH}}\right) * X_{AMB}$
	12) Lysis of XAMB
	$b_{AMB} * X_{AMB}$
	Acetotrophic sulfate reducing bacteria
	13) Growth of XASRB
	$\mu_{ASRB} * \left(\frac{S_A}{K_{SASRB} + S_A}\right) * \left(\frac{S_{SO4}}{K_{SOASRB} + S_{SO4}}\right) * \left(\frac{K_{H2SASRB}}{K_{H2SASRB} + S_{H2S^*}}\right) * \left(\frac{K_{OASRB}}{K_{OASRB} + S_O}\right) * \left(\frac{K_{NOASRB}}{K_{NOASRB} + S_{NO}}\right) * \left(\frac{S_{NH}}{K_{NHASRB} + S_{NH}}\right) * X_{ASRB}$
	14) Lysis of XASRB
	$b_{ASRB} * X_{ASRB}$
	Sulfide oxidizing bacteria
	15) Aerobic growth of XSOB on SH2S
	$\mu_{SOB} * \left(\frac{S_{H2S}}{K_{SSOB} + S_{H2S}}\right) * \left(\frac{S_O}{K_{OSOB} + S_O}\right) * \left(\frac{S_{NH}}{K_{NHSOB} + S_{NH}}\right) * X_{SOB}$
	16) Anoxic growth of XSOB on SH2S
	$\mu_{SOB} * \eta_{SOB} * \left(\frac{S_{H2S}}{K_{SSOB} + S_{H2S}}\right) * \left(\frac{S_{NO}}{K_{NOSOB} + S_{NO}}\right) * \left(\frac{K_{OSOB}}{K_{OSOB} + S_O}\right) * \left(\frac{S_{NH}}{K_{NHSOB} + S_{NH}}\right) * X_{SOB}$
	17) Lysis of XSOB
	$b_{SOB} * X_{SOB}$

measured values of porosity and saturated hydraulic conductivity (the '*Measured K_s + porosity*' parameter set), measured and simulated effluent flow rates match better; however, the peak of the effluent flow rate is overpredicted. Using the '*Fitted parameter set*', a good match between simulated and measured data can be achieved. This indicates that it is necessary to measure at least the porosity and the saturated hydraulic conductivity of the filter material to obtain reasonable simulation results for water flow.

Table 9.18 shows measured and simulated concentrations of ammonia and nitrate nitrogen (NH_4-N and NO_3-N, respectively) for the VF pilot-scale CWs with two

Table 9.15 Kinetic parameters in the CWM1 biokinetic model (Langergraber et al., 2009b).

Parameter	Description [unit]	Value
Hydrolysis		For 20 °C (10 °C)
K_h	Hydrolysis rate constant [1/d]	3 (2)
K_X	Saturation/inhibition coefficient for hydrolysis [g COD_{SF}/g COD_{BM}]	0.1 (0.22)
K_H	Correction factor for hydrolysis by fermenting bacteria [-]	0.1
Heterotrophic bacteria (aerobic growth and denitrification)		
μ_H	Maximum aerobic growth rate on SF and SA [1/d]	6 (3)
K_g	Correction factor for denitrification by XH [-]	0.8
b_H	Rate constant for lysis [1/d]	0.4 (0.2)
K_{OH}	Saturation/inhibition coefficient for SO [mg O_2/l]	0.2
K_{SF}	Saturation/inhibition coefficient for SF [mg COD_{SF}/l]	2
K_{SA}	Saturation/inhibition coefficient for SA [mg COD_{SA}/l]	4
K_{NOH}	Saturation/inhibition coefficient for SNO [mg N/l]	0.5
K_{NHH}	Saturation/inhibition coefficient for SNH (nutrient) [mg N/l]	0.05
K_{H2SH}	Saturation/inhibition coefficient for SH2S [mg S/l]	140
Autotrophic bacteria		
μ_A	Maximum aerobic growth rate on SNH [1/d]	1 (0.35)
b_A	Rate constant for lysis [1/d]	0.15 (0.05)
K_{OA}	Saturation/inhibition coefficient for SO [mg O_2/l]	1
K_{NHA}	Saturation/inhibition coefficient for SNH [mg N/l]	0.5 (5)
K_{H2SA}	Saturation/inhibition coefficient for SH2S [mg S/l]	140
Fermenting bacteria		
μ_{FB}	Maximum aerobic growth rate for XFB [1/d]	3 (1.5)
b_{FB}	Rate constant for lysis [1/d]	0.02
K_{OFB}	Saturation/inhibition coefficient for SO [mg O_2/l]	0.2
K_{SFB}	Saturation/inhibition coefficient for SF [mg COD_{SF}/l]	28
K_{NOFB}	Saturation/inhibition coefficient for SNO [mg N/l]	0.5
K_{NHFB}	Saturation/inhibition coefficient for SNH (nutrient) [mg N/l]	0.01
K_{H2SFB}	Saturation/inhibition coefficient for SH2S [mg S/l]	140
Acetotrophic methanogenic bacteria		
μ_{AMB}	Maximum aerobic growth rate on for XAMB [1/d]	0.085
b_{AMB}	Rate constant for lysis [1/d]	0.008
K_{OAMB}	Saturation/inhibition coefficient for SO [mg O_2/l]	0.0002
K_{SAMB}	Saturation/inhibition coefficient for SA [mg COD_{SA}/l]	56
K_{NOAMB}	Saturation/inhibition coefficient for SNO [mg N/l]	0.0005
K_{NHAMB}	Saturation/inhibition coefficient for SNH (nutrient) [mg N/l]	0.01
K_{H2SAMB}	Saturation/inhibition coefficient for SH2S [mg S/l]	140

(*Continued*)

Table 9.15 (Continued)

Parameter	Description [unit]	Value
Acetotrophic sulfate reducing bacteria		
μ_{ASRB}	Maximum aerobic growth rate for XASRB [1/d]	0.18
b_{ASRB}	Rate constant for lysis [1/d]	0.012
K_{OASRB}	Saturation/inhibition coefficient for SO [mg O_2/l]	0.0002
K_{SASRB}	Saturation/inhibition coefficient for SA [mg COD_{SA}/l]	24
K_{NOASRB}	Saturation/inhibition coefficient for SNO [mg N/l]	0.0005
K_{NHASRB}	Saturation/inhibition coefficient for SNH (nutrient) [mg N/l]	0.01
K_{SOASRB}	Saturation/inhibition coefficient for SSO4 [mg S/l]	19
$K_{H2SASRB}$	Saturation/inhibition coefficient for SH2S [mg S/l]	140
Sulfide oxidizing bacteria		
μ_{SOB}	Maximum aerobic growth rate for XSOB [1/d]	5.28
K_{SOB}^{*}	Correction factor for anoxic growth of XSOB [-]	0.8
b_{SOB}	Rate constant for lysis [1/d]	0.15
K_{OSOB}	Saturation/inhibition coefficient for SO [mg O_2/l]	0.2
K_{NOSOB}	Saturation/inhibition coefficient for SNO [mg N/l]	0.5
K_{NHSOB}	Saturation/inhibition coefficient for SNH (nutrient) [mg N/l]	0.05
K_{SSOB}	Saturation/inhibition coefficient for SH2S [mg S/l]	0.24

*Typing error in the original CWM1 publication.

different sandy filter materials used for the main layer. Besides the sand with a grain size of 0.06–4 mm, sand with a grain size of 1–4 mm was also tested. The different levels of the NO_3-N effluent concentrations for the two filter materials could be simulated. The effluent concentrations of NO_3-N for the 1-4 mm substrate have been higher, because less readily degradable organic matter is produced by hydrolysis that could be utilized for denitrification in deeper layers (Langergraber, 2003).

For the VF pilot-scale CWs with main layer of 0.06–4 mm sand, the distribution of microbial and bacterial biomass in different depths of the filter was also measured (Tietz et al., 2007). Converting the measured data into biomass COD results in mean values of 3400 to 5100 µg COD/g DW (dry weight of the substrate, i.e. sand) for the first centimetre of the main layer, 1100 to 2600 µg COD/g DW from 1–5 cm, and 640 to 1400 µg COD/g DW from 5–10 cm, respectively. Most of the biomass could be found in the upper 10 cm of the VF bed (Langergraber et al., 2007).

Simulated microbial biomass COD in the first centimetre of the main layer is between 5600 and 3400 µg COD/g DW (the range of the measured values) when using heterotrophic lysis rates of between 0.25 and 0.35 d^{-1}. Figure 9.3 compares calculated (from substrate-induced respiration) and simulated microbial biomass COD in different depths of the main layer for a heterotrophic lysis rate of 0.30 d^{-1}. When comparing measured and simulated biomass COD in different depths of the main layer, simulations seem to overpredict biomass COD in 1–5 cm depth and underpredict biomass COD in 5–10 cm depth. This could be an indication that the

Table 9.16 Temperature dependences, stoichiometric parameters, composition parameters and parameters describing oxygen transfer in the CW2D biokinetic model (Langergraber et al., 2009b).

Parameter	Description [unit]	Value
Temperature dependences (activation energy [J/mol] for Arrhenius equation)		
Tdep_HyKh	Activation energy hydrolyses [J/mol]	28,000
Tdep_HyKX	Activation energy factor KX for hydrolyses [J/mol]	–54,400
Tdep_H	Activation energy for processes caused by XH [J/mol]	47,800
Tdep_A	Activation energy for processes caused by XA [J/mol]	75,800
Tdep_KNHA	Activation energy for factor KNHA for nitrification [J/mol]	–160,000
Tdep_mueFB	Activation energy for XFB growth [J/mol]	47,800
Tdep_bFB	Activation energy for XFB lysis [J/mol]	0
Tdep_AMB	Activation energy for processes caused by XAMB [J/mol]	0
Tdep_ASRB	Activation energy for processes caused by XASRB [J/mol]	0
Tdep_SOB	Activation energy for processes caused by XSOB [J/mol]	0
Stoichiometric parameters		
$f_{Hyd,SI}$	Production of S_I in hydrolysis	0.0
$f_{BM,SF}$	Fraction of S_F generated in biomass lysis	0.05
$f_{BM,XI}$	Fraction of X_I generated in biomass lysis	0.1
Y_H	Yield coefficient for XH	0.63
Y_A	Yield coefficient for XA	0.24
Y_{FB}	Yield coefficient for XFB	0.053
Y_{AMB}	Yield coefficient for XAMB	0.032
Y_{ASRB}	Yield coefficient for XASRB	0.05
Y_{SOB}	Yield coefficient for XSOB	0.12
Composition parameters		
$i_{N,SF}$	N content of S_F [g N/g COD_{SF}]	0.03
$i_{N,SI}$	N content of S_I [g N/g COD_{SI}]	0.01
$i_{N,XS}$	N content of X_S [g N/g COD_{XS}]	0.04
$i_{N,XI}$	N content of X_I [g N/g COD_{XI}]	0.03
$i_{N,BM}$	N content of biomass [g N/g COD_{BM}]	0.07
Oxygen		
cO2_sat_20	Saturation concentration of oxygen [g/m^3]	9.18
Tdep_cO2_sat	Activation energy for saturation concentration of oxygen [J/mol]	–15,000
rate_O2	Re-aeration rate [1/d]	240

influence of biomass growth on the hydraulic properties has to be considered in the model (Langergraber et al., 2007).

Additionally, outdoor experiments were carried out at experimental CWs located at the wastewater treatment plant at Ernsthofen (Lower Austria). The experimental plant consisted of three parallel operating VF beds with a surface area of about 20 m^2 each.

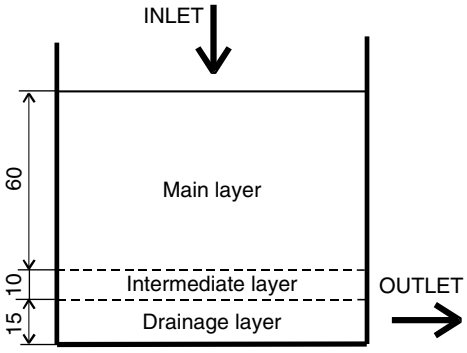

Figure 9.1 Schematic representation of the indoor pilot-scale CW (values are in cm).

Table 9.17 Soil hydraulic parameters of the van Genuchten-Mualem model for the 0.06–4 mm main layer (shape parameters α, N and L: van Genuchten, 1980).

Parameter	Residual water content ffj$_r$ (–)	Saturated water content ffj$_s$ (–)	Shape parameters α (cm^{-1})	N (–)	L (–)	Saturated hydraulic conductivity K_s (cm/h)
HYDRUS parameter set for 'Sand'	0.045	0.43	0.145	2.68	0.5	29.7
Measured K_s and porosity	0.045	0.30	0.145	2.68	0.5	117
Fitted parameter set	0.013	0.30	0.147	2.42	0.636	117

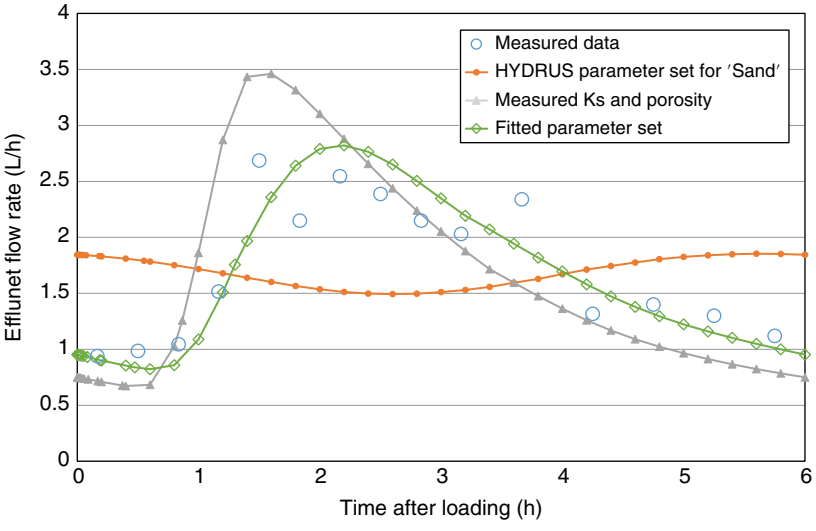

Figure 9.2 Measured and simulated effluent flow rates for a single feeding of 10 litres ('HYDRUS parameter set or Sand', 'Measured Ks and porosity' and 'Fitted parameter set' represent the parameter sets from Table 9.17).

Table 9.18 Median values of measured and simulated influent and effluent concentrations for NH_4-N and NO_3-N in mg/l (adapted from Langergraber, 2003).

	Influent	Effluent (0.06–4 mm sand)		Effluent (1–4 mm sand)	
Parameter	**Measured**	**Measured**	**Simulated**	**Measured**	**Simulated**
NH_4-N	60.0	0.15	0.01	1.20	0.16
NO_3-N	3.0	38.5	41.1	50.0	63.0

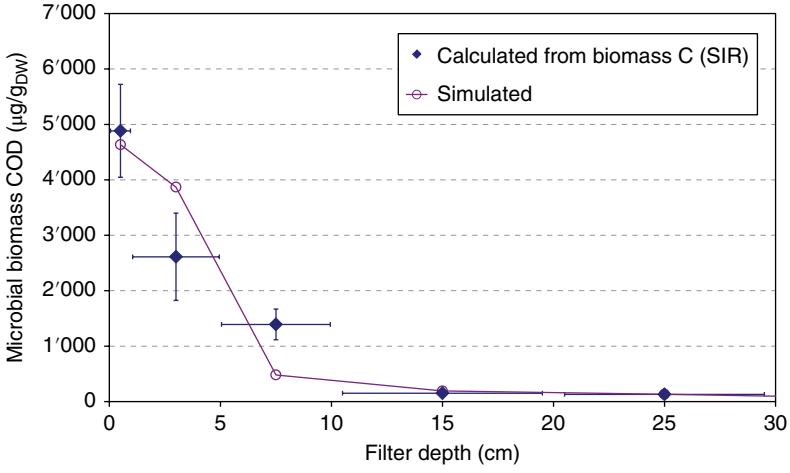

Figure 9.3 Calculated and simulated microbial biomass COD in different depths of the main layer (*Source:* adapted from Langergraber et al., 2007; Langergraber, 2015).

The organic loads for bed 1 to 3 were 20, 27 and 40 g COD/m^2/d, which correspond to hydraulic loading rates of 32.2, 43.0, and 64.7 mm/d. The main layer of the filter consisted of 50 cm sandy substrate (gravel size 0.06–4 mm, d_{10} = 0.2 mm; d_{60} = 0.8 mm). The beds are planted with common reed (*Phragmites australis*). The data gained from this experiment have been used to verify the temperature model incorporated into CW2D (Langergraber, 2007).

The width of the transport domain in the numerical simulations was 4 m, and its depth 0.8 m, while the transport domain itself was discretized into 31 columns and 33 rows. This resulted in a two-dimensional finite element mesh consisting of 1023 nodes and 1920 triangular finite elements. An atmospheric boundary condition was assigned to the top of the system representing the influent distribution system, and a constant pressure head boundary condition (constant head of –4 cm) was assigned to one side of the drainage layer (Langergraber, 2007).

Results for water flow comparing measured and simulated effluent flow rates and the cumulative effluent of the experimental CW are shown in Langergraber (2007). Simulated effluent flow rate and cumulative effluent flow match the measured data well.

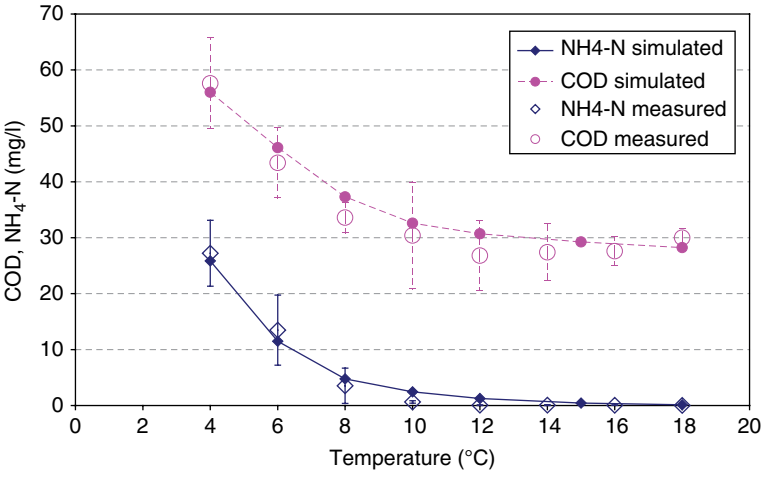

Figure 9.4 Measured and simulated COD and NH4-N effluent concentrations using the modified parameter set (adapted from Langergraber, 2007).

Using the calibrated flow model, the effluent concentrations during summer could be simulated using the standard CW2D parameter set (Langergraber and Šimůnek, 2005). However, measured COD and NH_4-N effluent concentrations at low temperatures could not be simulated because hydrolysis and nitrification at low temperatures were overpredicted. The standard CW2D parameter set considers temperature dependencies only for maximum growth, decay and hydrolysis rates. Figure 9.4 shows measured and simulated COD and NH_4-N effluent concentrations using a modified parameter set that includes temperature dependencies for the half-saturation constants of hydrolysis and nitrification. Using this modified parameter set, it was possible to simulate the COD and NH_4-N effluent concentrations at low temperatures (Langergraber, 2007).

9.5 Experiences and Challenges using Wetland Models

9.5.1 Description of Water Flow

It is generally agreed that the hydraulics have a high impact on the treatment performance of CWs. When simulating SSF CWs, the first step thus should be a good calibration of the water flow model. Experience shows that simulated effluent concentrations can match the measured data only when the hydraulic behaviour of the system is well described.

For VF CWs, the influence of the parameters describing the hydraulic properties of the filter material (such as for the van Genuchten-Mualem function in HYDRUS; Šimůnek et al., 2011) is much higher than the influence of the parameters of the biokinetic model. To achieve a good calibration of the water flow model, it is advised to measure at least the porosity and the saturated hydraulic conductivity of the filter material and, if possible, the volumetric effluent flow rate between two intermittent loadings (Langergraber, 2011). With these measurements, it is possible to estimate the remaining

parameters describing the hydraulic properties of the filter material using the inverse simulation implemented in HYDRUS (Šimůnek et al., 2011).

Morvannou et al. (2012) showed that macropores/cracks in some layers of a VF CW might serve as preferential flow paths through which water can bypass most of the soil porous matrix in a largely unpredictable way. This is especially true for the sludge layer in French-type VF CWs (Molle et al., 2005; Troesch and Esser, 2012). Water flow in such systems cannot be modeled with uniform flow models (such as using the Richards equation combined with the van Genuchten-Mualem function in HYDRUS; Šimůnek et al., 2011). The comparison between measured and simulated tracer breakthrough curves indicates that the nonequilibrium approach (i.e. using a model that separately describes flow and transport in preferred flow paths and slow or stagnant pore regions) seems to be more appropriate for simulating preferential flow. Such a dual-porosity model therefore also needs to be incorporated into the software tools to describe water flow and solute transport accurately in French VF CWs.

For HF CWs, in which the filter material is usually gravel and the saturated hydraulic conductivity is much larger than the actual water flow in the filter, tracer experiments are usually used to calibrate the water flow and single solute transport models.

9.5.2 Values of the Biokinetic Model Parameters and Influent Fractionation

Bacteria in CWs behave similarly to those in activated sludge systems. Based on this assumption, Langergraber (2001), when developing the first biokinetic model for CWs, proposed that parameters of the biokinetic models developed for activated sludge systems should be applicable to describe processes in CWs as well. This assumption was confirmed when it was shown that a good match between measured and simulated concentrations can be achieved when the hydraulic behaviour of the system is well described (see above). Additionally, Morvannou et al. (2011) found good agreement between measured and calculated volumetric nitrification rates (Table 9.19).

When using the biokinetic models such as CW2D or CWM1, it is therefore advised not to change the default parameters of the biokinetic model, except for good reasons. However, parameters characterizing the wastewater are related to the chosen biokinetic model. Influent fractionation has a high impact on the simulation results and needs to be adapted for each simulation study. These parameters include (1) fractionation of influent COD (i.e. estimation of different COD model fractions from measured total COD) and (2) organic N content of different COD fractions.

Table 9.19 Comparison of measured and calculated volumetric nitrification rates (adapted from Morvannou et al., 2011).

Method	Measured with solid respirometry	Calculated from simulation results*
Results [mg $O_2/l_{sample}/h$]	32–50 (mean = 41, SD = 9; 2 values)	30.5

*From simulations using parameters for the biokinetic model from activated sludge systems.

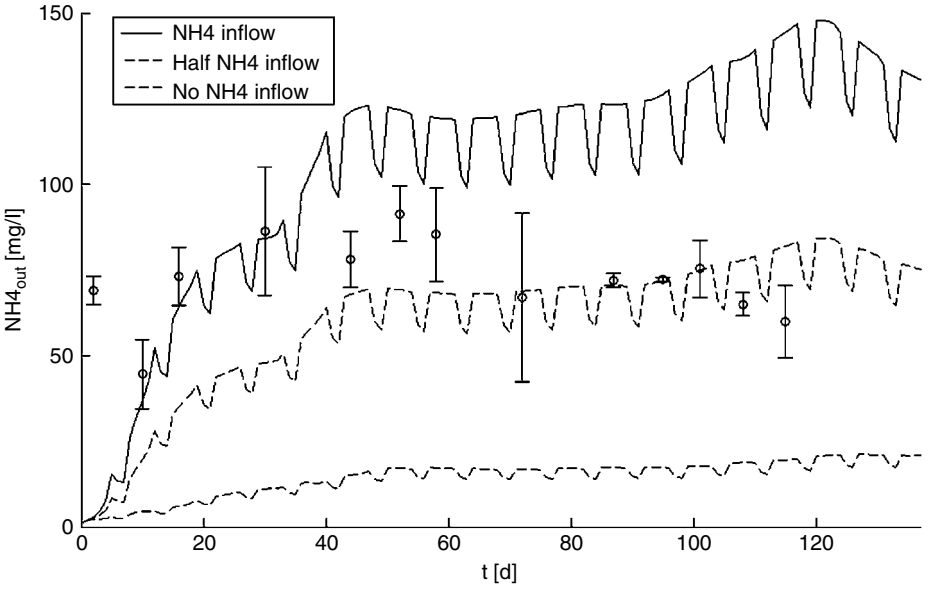

Figure 9.5 Influence of inflow NH_4-N concentrations on effluent NH_4-N concentrations (adapted from Langergraber and Morvannou, 2014).

Rizzo et al. (2014) described the setup of a model to simulate experimental data from a HF CW fed with artificial wastewater. During the experiments, the only nitrogen parameter measured in influent was TKN (Total Kjehldal Nitrogen). As the model requires influent concentrations of ammonia nitrogen, the organic N content of different COD fractions had to be adapted from standard values for the type of used artificial wastewater. This results in different ratios of ammonia nitrogen to TKN. Figure 9.5 shows the impact of different influent concentrations of ammonia nitrogen on simulated effluent concentrations. When all influent TKN is assumed to be ammonia (i.e. no organic nitrogen is present), simulated effluent concentrations of ammonia nitrogen are higher than measured effluent concentrations. In contrast, when all influent TKN is assumed to be organic nitrogen (i.e. no ammonia is present), simulated effluent concentrations are too low.

Pucher and Langergraber (2015) simulated vertical flow filters treating domestic wastewater using experimental data from Dal Santo et al. (2010). The main layer of the filters consisted of sand with a grain size of 1–4 mm or zeolite with a grain size of 2–5 mm. Both filters had an impounded drainage layer. After calibrating the flow model for the sand and zeolite filters (Table 9.20), the procedure for calibrating the biokinetic model was as follows: the standard parameter set of the CW2D biokinetic model (Langergraber and Šimůnek, 2012) was used in the first simulation of the sand filter ('simulated sand 1' in Table 9.21). This resulted in overprediction of nitrification, that is, simulated ammonia nitrogen concentrations were much lower than measured data. After reducing the maximum nitrification rate from 0.9 to 0.175 d^{-1}, the simulated effluent concentrations of ammonia nitrogen matched measured data well ('simulated sand 2' in Table 9.21). After adding the measured adsorption isotherms according to Dal Santo et al. (2010) and a first-order rate coefficient for nonequilibrium adsorption

Table 9.20 Estimated soil hydraulic parameters of the van Genuchten-Mualem model (shape parameters α, N and L: van Genuchten, 1980).

Parameter	Residual water content θ_r (–)	Saturated water content θ_s (–)	Shape parameters			Saturated hydraulic conductivity K_s (cm/min)
			α (cm^{-1})	N (–)	L (–)	
Sand (1–4 mm)	0.063	0.37	0.124	3.2	0.49	55
Zeolite (2–5 mm)	0.045	0.42	0.096	4.6	1.27	154

Table 9.21 Measured and simulated influent and effluent concentrations (in mg/l, measured data: average values and standard deviations in brackets, simulated data: average values over 1 day).

Parameter		CR	CS	CI	COD	NH_4-N	NO_2-N	NO_3-N
Influent	Measured	–	–	–	294	93	0.008	0.59
	Simulated	274	100	20	–	93	0.008	0.59
Effluent (sand)	Measured	–	–	–	**35 (5)**	**14.5 (4.6)**	0.026 (0.040)	**70.8 (8.4)**
	Simulated sand 1	0.17	0.08	31.2	31.5	0.42	<0.003	85.7
	Simulated sand 2	0.14	0.01	29.4	**30.0**	**15.3**	0.016	**76.2**
Effluent (zeolite)	Measured	–	–	–	**29 (9)**	**0.06 (0.05)**	0.52 (1.10)	**51.8 (4.6)**
	Simulated zeolite	0.16	0.01	29.1	**29.3**	**0.27**	<0.003	**43**

of 0.01 d^{-1}, a good match between simulated and measured data could be obtained for the zeolite filter ('simulated zeolite' in Table 9.21).

Pálfy and Langergraber (2014) simulated experimental results from batch-fed column experiments using the CWM1 biokinetic model. They described the need to adjust some parameters of the biokinetic model to be able to simulate anaerobic, anoxic, and aerobic processes to occur in parallel. These phenomena occurred in practice and can be explained by the local effect of root zone re-aeration. Figure 9.6 shows measured and simulated sulfate concentrations before and after the adjustment of parameters of the biokinetic model. Batch experiments can be used to calibrate the biokinetic model parameters as there is no impact of water flow on the treatment performance.

9.5.3 Clogging Model

Modeling of clogging processes is not possible using the HYDRUS Wetland module. Langergraber and Šimůnek (2009) coupled the colloids attachment/detachment model according to Bradford et al. (2003) (implemented in the standard HYDRUS module) with the CW2D biokinetic model. It was assumed that CS, the slowly biodegradable organic matter (as defined by Langergraber and Šimůnek, 2005), consists of a particulate matter XS that can be divided into five different classes according to different

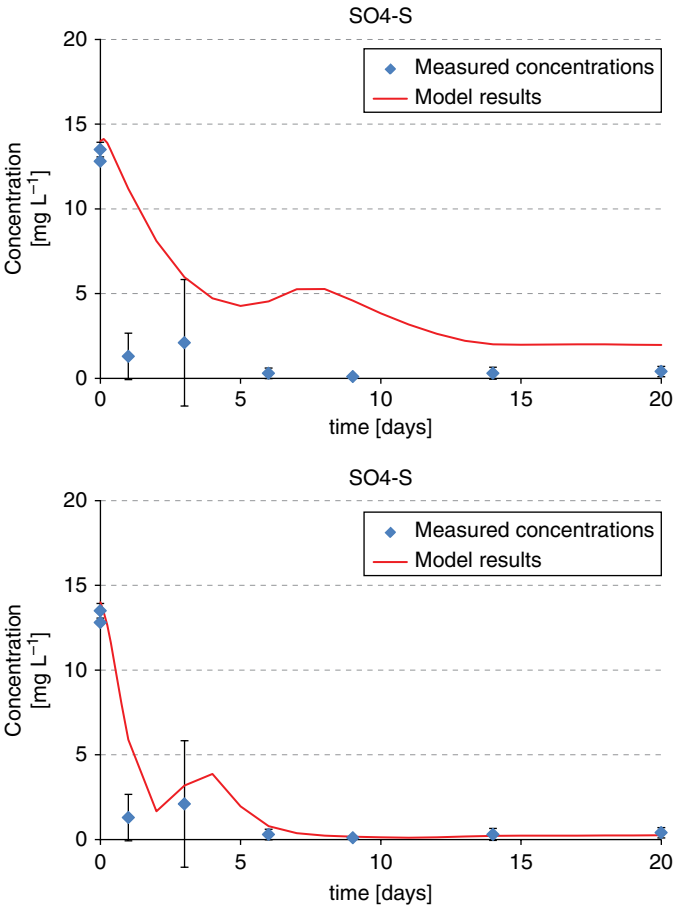

Figure 9.6 Measured and simulated sulfate concentrations for a batch-fed column at 24 °C planted with *Carex* (left: with the standard parameter set of the biokinetic model; right: after adjusting inhibition and half-saturation coefficients to allow anaerobic, anoxic, and aerobic processes to occur in parallel). Adapted from Pálfy (2013).

particle sizes (<1, 1–3, 3–10, 10–30, and 30–100 µm, respectively). It was further assumed that particles are transported in the liquid phase until they are attached. Once attached the particles undergo hydrolysis and cCR (readily biodegradable organic matter; Langergraber and Šimůnek, 2005) in the liquid phase is produced. An additional assumption was that particles with different sizes have the same density and degradability.

The model was tested using measurements of particle concentrations in different depths within the 50-cm main layer of the VF pilot-scale CW, as described earlier. Particle measurements at the inlet were used to calculate fractionation of COD influent. Measured and simulated soluble particulate COD concentrations for the 10–30 µm particle class before and after loading of the VF filter along the filter depth are shown in Figure 9.7. 'Measured' COD was derived from particle measurements. In general, the

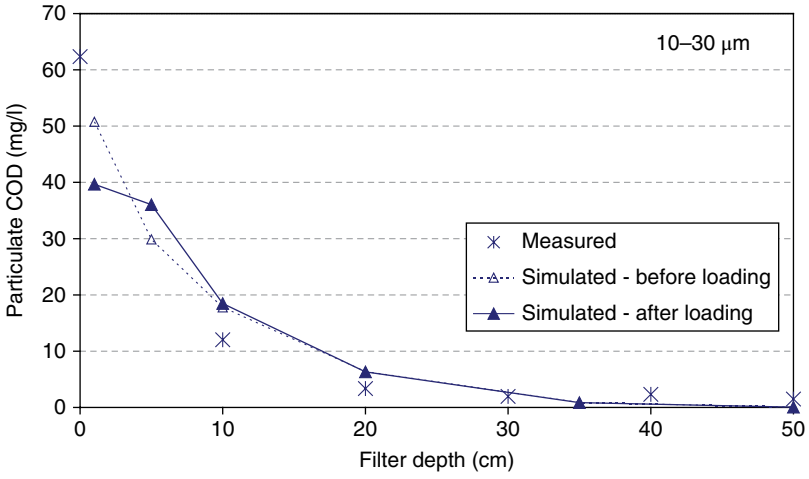

Figure 9.7 Comparison of measured and simulated particulate COD for the 10–30 µm particle class (adapted from Langergraber and Šimůnek, 2009).

first test showed a good agreement between measured and simulated particulate COD. However, there is still a great need for further testing of the particle transport model and for finding an optimal parameter set for various conditions present in constructed wetlands.

Several clogging models have been developed for BIO_PORE (Samsó and García, 2013). Samsó and García (2014) described the relationship between bacterial communities and accumulated solids, leading to clogging in a HF CW. The so-called 'Cartridge Theory' describes how the active bacterial zone moves in the filter. In this model, the effect of the inert organic matter accumulated in pores upon the hydraulic conductivity is not considered. Description of limited growth of bacteria was implemented by adding two parameters. The first parameter provides a negative feedback term to the growth of all bacteria groups to prevent their unlimited growth in areas where substrate concentrations are high (which is especially relevant for the influent zones of HF CWs). The second parameter provides a negative feedback term to the growth equations, but in this case, it decreases the growth rate of bacteria due to progressive accumulation of inert solids in the pore space of the granular media. Samsó et al. (2015a) described in their simulation study the effect of bacteria density and accumulated inert solids on effluent pollutant concentrations, but again only without considering the effect of organic matter accumulation on water flow. Samsó et al. (2016) additionally described the effects of a pore size reduction on the hydraulic conductivity using the biological clogging model proposed by Mostafa and Van Geel (2007). Using this approach, Samsó et al. (2016) were able to simulate realistic behaviour of HF CWs, including overland flow and re-infiltration of water in the unused filter material.

9.5.4 Models as CW Design Tools

Langergraber (2011) concluded that further developments of existing models are needed to make them a useful and applicable tool for a CW design. A simplified

computer-based CW design tool, based on process-based numerical models, should be developed that:

- could be used with knowledge about a CW design, but without requiring special knowledge about numerical modeling;
- allows designing CWs for different boundary conditions (such as different climatic conditions, wastewater characterization, filter material, etc.); and
- makes the description of the dynamic behaviour of the designed CW possible, thus allowing demonstration of the greater robustness of CW treatment systems, for example, for fluctuating inflows and peak loads.

Several advances have been made to develop such a simplified design tool. Meyer and Dittmer (2015) developed RSF_Sim, which supports the design of CWs for a combined sewer overflow treatment: retention soil filters (RSFs). This simplified, yet robust and reliable, model was developed for design purposes based on experiences with the HYDRUS Wetland module. RSF_Sim has only a few parameters and is therefore simple to use. RSF_Sim was developed specifically for RSFs for German conditions. Pálfy et al. (2015b) adapted RSF_Sim for CWs for a combined sewer overflow treatment for French conditions (e.g. for different design rules and effluent requirements).

A similar approach was taken by Morvannou et al. (2015). The aim of their work was to develop a simple model to support the design of French-type VF CWs. Numerical simulation using the HYDRUS Wetland module were first performed, varying a number of design parameters. The design parameters included the depth of the main layer of the first-stage filter, the hydraulic loading rate, and the inlet COD concentration and temperature. Effluent concentration of the first-stage filter was then verified using measured data and a surrogate model was developed to estimate COD and NH_4-N removal in relation to the design parameters. Although the first results were promising, Morvannou et al. (2015) concluded that more work needs to be done to develop a robust design model.

9.6 Summary and Conclusions

Interest in modeling processes in CWs has increased over the last 15 years. Several mechanistic models to describe processes in subsurface flow CWs have been developed. However, the HYDRUS Wetland module is the only one that is commercially available and thus available for wider use.

Experiences with applying the HYDRUS Wetland module and other existing simulation tools can be summarised as follows:

- Simulation studies often suffer from a lack of data. When the use of dynamic models is anticipated, experiments have to be planned in a way that data for model calibration and validation are available. Data requirements are different for different models, but always include careful planning of sampling frequency and analysed parameters (Meyer et al., 2015). The amount and nature of data needed for calibration depends on the objectives of the simulation study. In general, for calibration of the water flow model, more data are required for vertical flow CWs compared with horizontal flow CWs. The amount of data required for calibrating reactive transport simulations

depends on biokinetic model parameters (e.g. influent fractionations), as well as the dynamics of influent in the system.

- Good calibration of the water flow model is a prerequisite for achieving a good match between measured and simulated pollutant concentrations. If the water flow model is calibrated, good results can be obtained in most applications when using the standard parameter sets of the biokinetic CW2D and CWM1 models (Langergraber and Šimůnek, 2012). Influent fractionation (i.e. fractionation of influent COD and the N and P contents of different COD fractions) has a high impact on simulation results and thus is an essential part of calibrating reactive transport models. This is especially true when simulating CWs treating other than domestic wastewater.
- One of the main obstacles for the wider use of available simulation tools is that they are rather complicated and difficult to run. Simplified, yet robust and reliable, models for the design of CWs need to be developed (such as RSF_Sim, developed to support the design of CWs treating combined sewer overflow; Meyer and Dittmer, 2015).

References

Bradford, S.A., Šimůnek, J., Bettahar, M., et al. (2003). Modeling colloid attachment, straining, and exclusion in saturated porous media. *Environmental Science and Technology* 37 (10): 2242–2250.

Dal Santo, S., Canga, E., Pressl, A., et al. (2010). Investigation of nitrogen removal in a two-stage subsurface vertical flow constructed wetland system using natural zeolite. In: *Proceedings of the 12th IWA Specialized Group Conference on Wetland Systems for Water Pollution Control* (ed. F. Masi and J, Nivala), 263–270. 3–8 October 2010, San Servolo, Venice, Italy.

Dittmer, U., Meyer, D., and Langergraber, G. (2005). Simulation of a subsurface vertical flow constructed wetland for CSO treatment. *Water Science and Technology* 51 (9): 225–232.

García, J., Rousseau, D.P.L., Morató, J., et al. (2010). Contaminant removal processes in subsurface-flow constructed wetlands: a review. *Critical Reviews in Environmental Science and Technology* 40 (7): 561–661.

Henrichs, M., Langergraber, G., and Uhl, M. (2007). Modelling of organic matter degradation in constructed wetlands for treatment of combined sewer overflow. *Science of the Total Environment* 380 (1–3): 196–209.

Henrichs, M., Welker, A., Uhl, M. (2009). Modelling of biofilters for ammonium reduction in combined sewer overflow. *Water Science and Technology* 60 (3), 825–831.

Kadlec, R.H. and Wallace, S. (2009). *Treatment Wetlands*, 2nd ed. Boca Raton, FL: CRC Press.

Karlsson, S.C., Langergraber, G., Pell, M., et al. (2015). Simulation and verification of hydraulic properties and organic matter degradation in sand filters for greywater treatment. *Water Science and Technology* 71 (3): 426–433.

Kumar, J.L.G. and Zhao, Y.Q. (2011). A review on numerous modeling approaches for effective, economical and ecological treatment wetlands. *Journal of Environmental Management* 92: 400–406.

Langergraber, G. (2001). *Development of a simulation tool for subsurface flow constructed wetlands*. PhD dissertation, BOKU University, Vienna, Austria.

Langergraber, G. (2003). Simulation of subsurface flow constructed wetlands – Results and further research needs. *Water Science and Technology* 48 (5): 157–166.

Langergraber, G. (2007). Simulation of the treatment performance of outdoor subsurface flow constructed wetlands in temperate climates. *Science of the Total Environment* 380 (1–3): 210–219.

Langergraber, G. (2008). Modeling of processes in subsurface flow constructed wetlands – A review. *Vadose Zone Journal* 7 (2): 830–842.

Langergraber, G. (2011). Numerical modelling: A tool for better constructed wetland design? *Water Science and Technology* 64 (1): 14–21.

Langergraber, G. (2015). *Erratum: Water Science and Technology* 56 (3), 2007, 233–240: Comparison of measured and simulated distribution of microbial biomass in subsurface vertical flow constructed wetlands. *Water Science and Technology* 71 (1): 157–158.

Langergraber, G. and Šimůnek, J. (2005). Modeling variably-saturated water flow and multi-component reactive transport in constructed wetlands. *Vadose Zone Journal* 4 (4): 924–938.

Langergraber, G. and Šimůnek, J. (2009). Simulating particle transport in subsurface flow constructed wetlands with CW2D/HYDRUS. In: *3rd International Symposium on Wetland Pollutant Dynamics and Control – WETPOL 2009 Book of Abstracts* (ed. J.M. Bayona and J. García), 135–136. Barcelona, 20–24 September 2009.

Langergraber, G. and Šimůnek, J. (2011). *HYDRUS Wetland Module, Version 2, Manual*. Hydrus Software Series 4, Department of Environmental Sciences, University of California Riverside, Riverside, CA.

Langergraber, G. and Šimůnek, J. (2012). Reactive transport modeling of subsurface flow constructed wetlands using the HYDRUS Wetland module. *Vadose Zone Journal* 11 (2): Special Issue on Reactive Transport Modeling. doi:10.2136/vzj2011.0104

Langergraber, G. and Morvannou, A. (2014). Modelling of treatment wetlands. *Sustainable Sanitation Practice* 18 (January 2014): 31–36. Available at www.ecosan.at/ssp

Langergraber, G., Tietz, A., and Haberl, R. (2007). Comparison of measured and simulated distribution of microbial biomass in subsurface vertical flow constructed wetlands. *Water Science and Technology* 56 (3): 233–240.

Langergraber, G., Giraldi, D., Mena, J., et al. (2009a). Recent developments in numerical modelling of subsurface flow constructed wetlands. *Science of the Total Environment* 407 (13): 3931–3943.

Langergraber, G., Rousseau, D., García, J., and Mena, J. (2009b). CWM1 – A general model to describe biokinetic processes in subsurface flow constructed wetlands. *Water Science and Technology* 59 (9): 1687–1697.

Mburu, N., Sanchez-Ramos, D., Rousseau, D.P.L., et al. (2012). Simulation of carbon, nitrogen and sulphur conversion in a batch-operated experimental wetland mesocosm. *Ecological Engineering* 42: 304–315.

Meyer, D. (2011). Modellierung und Simulation von Retentionsbodenfiltern zur weitergehenden Mischwasserbehandlung [Modelling and simulation of constructed wetlands for treatment of combined sewer overflow]. PhD thesis, Technical University of Kaiserslautern, Germany. Available at https://kluedo.ub.uni-kl.de/frontdoor/index/index/docId/2843

Meyer D. and Dittmer U. (2015). RSF_Sim – A simulation tool to support the design of constructed wetlands for combined sewer overflow treatment. *Ecological Engineering* 80: 198–204.

Meyer, D., Chazarenc, F., Claveau-Mallet, D., et al. (2015). Modelling constructed wetlands: Scopes and aims – A comparative review. *Ecological Engineering* 80: 205–213.

Molle, P., Liénard, A., Boutin, C., et al. (2005). How to treat raw sewage with constructed wetlands: an overview of the French systems. *Water Science and Technology* 51 (9): 11–21.

Morvannou, A., Choubert, J.-M., Vanclooster, M., and Molle, P. (2011). Solid respirometry to characterize nitrification kinetics: A better insight for modelling nitrogen conversion in vertical flow constructed wetlands. *Water Research* 45 (16): 4995–5004.

Morvannou, A., Forquet, N., Vanclooster, M., and Molle, P. (2012). Which hydraulic model to use in vertical flow constructed wetlands? *Proceedings of the 13th IWA Specialized Group Conference on Wetland Systems for Water Pollution Control* – Conference Papers Volume 2, 145–153. 25–29 November 2012, Perth.

Morvannou, A., Froquet, N., Troesch, S., and Molle, P. (2015). Impact of design and operating conditions on vertical flow constructed wetland performances: modelling and global assessment confrontation. *6th International Symposium on Wetland Pollution Dynamics and Annual Conference of the Constructed Wetland Association* – Book of Abstracts, 196–197. 13–18 September 2015, York, UK.

Mostafa, M. and Van Geel, P.J. (2007). Conceptual models and simulations for biological clogging in unsaturated soils. *Vadose Zone Journal* 6: 175–185.

Pálfy, T. (2013). *Verification of the implementation of CWM1 in the HYDRUS wetland module*. MSc thesis, BOKU University, Vienna, Austria.

Pálfy, T.G. and Langergraber, G. (2014). The verification of the Constructed Wetland Model No. 1 implementation in HYDRUS using column experiment data. *Ecological Engineering* 68: 105–115.

Pálfy, T.G., Gribovszki, Z., and Langergraber, G. (2015a). Design-support and performance estimation using HYDRUS/CW2D: A horizontal flow constructed wetland for polishing SBR effluent. *Water Science and Technology* 71 (7): 965–970.

Pálfy, T.G., Meyer, D., and Molle, P. (2015b). Orage: Simulation of planted detentive filters treating urban storm water. *6th International Symposium on Wetland Pollution Dynamics and Annual Conference of the Constructed Wetland Association* – Book of Abstracts, 216–217. 13–18 September 2015, York, UK.

Pucher, B. and Langergraber, G. (2015). Simulation of two-stage vertical flow sand and zeolite filters treating domestic wastewater using the HYDRUS wetland module. *6th International Symposium on Wetland Pollution Dynamics and Control and Annual Conference of the Constructed Wetland Association* – Book of Abstracts, 198–199. 13–18 September 2015, York, UK.

Rizzo, A., Langergraber, G., Galváo, A., et al. (2014). Modelling the response of horizontal flow constructed wetlands to unsteady organic loads with HYDRUS-CWM1. *Ecological Engineering* 68: 209–213.

Samsó, R. and Garcia, J. (2013). BIO PORE, a mathematical model to simulate biofilm growth and water quality improvement in porous media: Application and calibration for constructed wetlands. *Ecological Engineering* 54: 116–127.

Samsó, R. and García, J. (2014). The Cartridge Theory: A description of the functioning of horizontal subsurface flow constructed wetlands for wastewater treatment, based on modelling results. *Science of The Total Environment* 473–474: 651–658.

Samsó, R., Blázquez, J., Agulló, N., et al. (2015a). Effect of bacteria density and accumulated inert solids on the effluent pollutant concentrations predicted by the constructed wetlands model BIO_PORE. *Ecological Engineering* 80: 172–180.

Samsó, R., Meyer, D., and García, J. (2015b). Subsurface flow constructed wetland models: review and prospects. In: *The Role of Natural and Constructed Wetlands in Nutrient Cycling and Retention on the Landscape* (ed. J. Vymazal), 149–174. Springer International Publishing.

Samsó, R., García, J., Molle, P., and Forquet, N. (2016). Modelling bioclogging in variably saturated porous media and the interactions between surface/subsurface flows: application to Constructed Wetlands. *Journal of Environmental Management* 165: 271–279.

Šimůnek, J., van Genuchten, M.Th., and Šejna, M. (2008). Development and applications of the HYDRUS and STANMOD software packages and related codes. *Vadose Zone Journal* 7 (2): 587–600.

Šimůnek J., Šejna, M., and van Genuchten, M.Th. (2011). *The HYDRUS Software Package for Simulating the Two- and Three-Dimensional Movement of Water, Heat, and Multiple Solutes in Variably-Saturated Media*. Technical Manual, Version 2.0. PC-Progress, Prague.

Šimůnek, J., Jacques, D., Langergraber, G., et al. (2013). Numerical modeling of contaminant transport using HYDRUS and its specialized modules. *Journal of the Indian Institute of Science* 93 (2): 265–284.

Smethurst, P.J, Petrone, K., Langergraber, G., et al. (2014). Nitrate dynamics in a rural headwater catchment: measurements and modeling. *Hydrological Processes* 28 (4): 1820–1834.

Tietz, A., Langergraber, G., Sleytr, K., et al. (2007). Characterization of microbial biocoenosis in vertical subsurface flow constructed wetlands. *Science of the Total Environment* 380 (1–3): 163–172.

Toscano, A., Langergraber, G., Consoli, S., and Cirelli, G.L. (2009). Modelling pollutant removal in a pilot-scale two-stage subsurface flow constructed wetlands. *Ecological Engineering* 35 (2): 281–289.

Troesch, S. and Esser, D. (2012). Constructed wetlands for the treatment of raw wastewater: The French experience. *Sustainable Sanitation Practice* 12 (July 2012): 9–15. Available at www.ecosan.at/ssp

van Genuchten, M.Th. (1980). A closed form equation for predicting the hydraulic conductivity of unsaturated soils. *Soil Science Society of America Journal* 44: 892–898.